

# High-Precision Schottky Diagnostics for Low-SNR Betatron Tune Measurement in Ramping Synchrotrons

Peihan Sun\*

*Shanghai Institute of Applied Physics, Chinese Academy of Sciences, Shanghai 201800, China and  
University of Chinese Academy of Sciences*

Manzhou Zhang†

*Shanghai Institute of Applied Physics, Chinese Academy of Sciences, Shanghai 201800, China and  
Shanghai Advanced Research Institute, Chinese Academy of Sciences, Shanghai 201204, China*

Renxian Yuan

*Shanghai Institute of Applied Physics, Chinese Academy of Sciences, Shanghai 201800, China and  
Shanghai Advanced Research Institute, Chinese Academy of Sciences, Shanghai 201204, China*

Deming Li

*Shanghai Institute of Applied Physics, Chinese Academy of Sciences, Shanghai 201800, China*

Jian Dong

*Shanghai Advanced Research Institute, Chinese Academy of Sciences, Shanghai 201204, China*

Ying Shi

*Shanghai Institute of Applied Physics, Chinese Academy of Sciences, Shanghai 201800, China and  
University of Chinese Academy of Sciences*

(Dated: December 30, 2024)

This paper presents a novel Schottky diagnostics-based method for real-time betatron tune measurement in ramping synchrotrons, exemplified by the Shanghai Advanced Proton Therapy (SAPT) facility. The proposed approach achieves high precision under challenging conditions, including low frequency resolution and signal-to-noise ratios (SNR) as low as -15 dB within the bandwidth of a narrowband detector. By employing Short-Time Fourier Transform (STFT) analysis with automatically optimized time windows, the method effectively addresses the rapid increase in revolution frequency from 4 MHz to 7.5 MHz over 0.35 seconds, assuming constant beam properties within each window. Monte Carlo macro-particle simulations are employed to generate Schottky signals, which are subsequently combined with real noise collected from an analog-to-digital converter to emulate practical conditions. The betatron tune measurement procedure integrates longitudinal signal exclusion, spectrum smoothing, and spectral multiplication to reliably extract transverse Schottky spectra buried in noise, to enable precise betatron tune determination. Experimental results demonstrate that the proposed method surpasses existing approaches in precision, accuracy, and robustness, while meeting stringent design requirements. This innovative approach addresses key limitations of Schottky diagnostics for betatron tune measurement in ramping synchrotrons, providing a foundation for applications such as proton therapy.

## I. INTRODUCTION

To optimize the third-order resonance slow extraction of the Shanghai Advanced Proton Therapy (SAPT) facility [1], the main ring must be capable of performing betatron tune measurements under different energy and bunching or drifting beam. However, due to the absence of an integrated design for the betatron tune measurement system, the current setup can only measure the tune while bunching. Based on the practical experience of the SAPT facility, the residual oscillations after injection do not seem to be effectively sustained, mak-

ing it difficult to obtain a coherent tune signal from the beam position monitor (BPM) data. This process involves using a slow extraction kicker for excitation, followed by applying a Fast Fourier Transform (FFT) to signals from the BPM. Additionally, excitation evidently interferes with the extraction process. This limitation hinders the system from meeting the demands of further optimization. Therefore, a feasible option at present is to perform tune measurements by obtaining the incoherent transverse oscillation signal, specifically using the Schottky signal measurements method.

Since the invention of the stochastic cooling concept by Simon van der Meer in 1972 [2], Schottky signal measurements have been widely used as a non-invasive tool for the determination of beam properties, such as momentum spread, betatron tune, synchrotron frequency, and chromaticity. In practice, reaching a high SNR has

\* sunpeihan22@mailsucas.ac.cn

† Contact author: zhangmanzhou@sinap.ac.cn

always been challenging. The SNR of the measured signal is affected by factors such as the longitudinal length of the pick-up, the sensitivity of the BPM, and the working frequency of the system. Consequently, the design and manufacturing of the pick-up may be constrained by various objective factors, making it challenging to ensure a high SNR. Furthermore, the variable revolution frequency and betatron tune during ramping progress and extraction energy make it impractical to perform a windowed spectrum overlapping procedure to increase SNR, as has been done in previous work by CERN [3]. Given these limitations, an alternative approach is required to measure the betatron tune of the SAPT facility.

In this paper, we identify the method and procedure for measuring the betatron tune under the conditions of original signal with low SNR, varying revolution frequency, and fluctuating. We incorporate simulated signals at different revolution frequencies, betatron tune and sampling rates into real-world noise collected from an analog-to-digital converter (ADC) to evaluate the reliability and general applicability of this method. Depending on the signal quality and specific requirements, different types of spectral smoothing techniques can be employed to achieve a trade-off between processing time and precision.

The paper is organized as follows. Details of the time-domain Schottky signal simulation are provided in Sections II A, II B, and II C, including the parameters of the synchrotron and considerations prior to the simulation. In Section II D, we describe how the simulated signal is combined with real-world noise to achieve the desired SNR. Section III outlines the criteria and considerations for determining key parameters, including the ADC sampling rate and the optimal window size for performing the Short-Time Fourier Transform (STFT) while minimizing spectral distortion. Section IV introduces a key innovation of this paper: a novel betatron tune measurement procedure tailored for ramping synchrotrons operating under low SNR conditions. The method begins by excluding the longitudinal signal spectrum to focus solely on the transverse Schottky signal, an essential step for precise tune measurements. Advanced spectrum smoothing techniques are then applied, followed by spectral multiplication to amplify the visibility of the transverse Schottky signal buried in noise. This step is critical for accurately identifying the shape and position of the transverse signal under challenging conditions. Finally, a robust tune calculation method is implemented, employing Gaussian fitting to achieve high-precision determination of the betatron tune. In Section V, we validate the general applicability of the proposed method under various conditions. We compare the average absolute error of the measured tune relative to the nominal fractional tune, the standard deviation of the measured tune, and the precision of the measured tune achieved by different betatron tune measurement methods. Finally, concluding remarks are provided in Section VI.

## II. MACRO-PARTICLE MONTE CARLO SIMULATION

### A. Longitudinal Schottky Spectrum

The longitudinal Schottky time-domain signal of  $N$  particles in a bunched beam of proton synchrotron at the  $n$ -th harmonic can be shown [3–8] to be given by

$$\begin{aligned} I(t) &= 2ef_0 \sum_{i=1}^N \cos(n\omega_0(t + \hat{\tau}_i \sin(\Omega_s t + \psi_i))) \quad (1) \\ &= 2ef_0 \sum_{i=1}^N \sum_{p=-\infty}^{\infty} J_p(n\omega_0 \hat{\tau}_i) \cos(n\omega_0 t + p\Omega_s t + p\psi_i) \quad (2) \end{aligned}$$

where  $e$  is the elementary charge,  $f_0$  is the nominal revolution frequency,  $\omega_0 = 2\pi f_0$  is the angular nominal revolution frequency in radians,  $\hat{\tau}_i$  is the synchrotron oscillation amplitude of particle  $i$ ,  $\Omega_{s_i} = 2\pi f_{s_i}$  is the angular synchrotron frequency of particle  $i$ ,  $\psi_i$  is the initial synchrotron phase, and  $J_p$  is the Bessel function of the first kind of order  $p$ .

The nominal bunch length is about one-quarter of the circumference of the ring according to the RF voltage. The synchrotron oscillation amplitude of particle  $i$ ,  $\hat{\tau}_i$ , follows a Gaussian distribution centered at zero with  $\sigma = T/16$ , where  $T = 1/f_0$  represents the period in STFT time window. The synchrotron frequency of particle  $i$  depends solely on the synchrotron oscillation amplitude and follows from the solution of the pendulum equation [6], yielding:

$$\Omega_{s_i} = \frac{\pi}{2K(\sin(\frac{\omega_{RF} \hat{\tau}_i}{2}))} \Omega_{s_0} \quad (3)$$

where  $K([0, 1]) \rightarrow [\frac{\pi}{2}, \infty)$  is the complete elliptic integral of the first kind,  $\omega_{RF} = 1 \cdot \omega_0$  is the RF frequency, and  $\Omega_{s_0} = q_s \cdot \omega_0$  is the zero-amplitude synchrotron frequency, where  $q_s$  represents the synchrotron tune. The initial synchrotron phase of particle  $i$ ,  $\psi_i$ , is drawn from a uniform distribution over the range  $(-\pi, \pi)$ . The longitudinal shape of  $10^4$  macro-particles power spectral density (PSD) under SAPT conditions is shown in Fig. 1.

### B. Transverse Schottky Spectrum

The transverse dipole Schottky time-domain signal of  $N$  particles in a bunched beam of proton synchrotron at the  $n$ -th harmonic can be shown [3–5, 8, 9] to be repre-

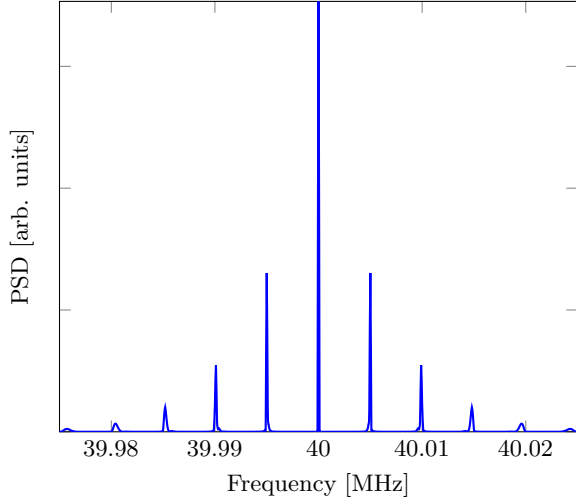


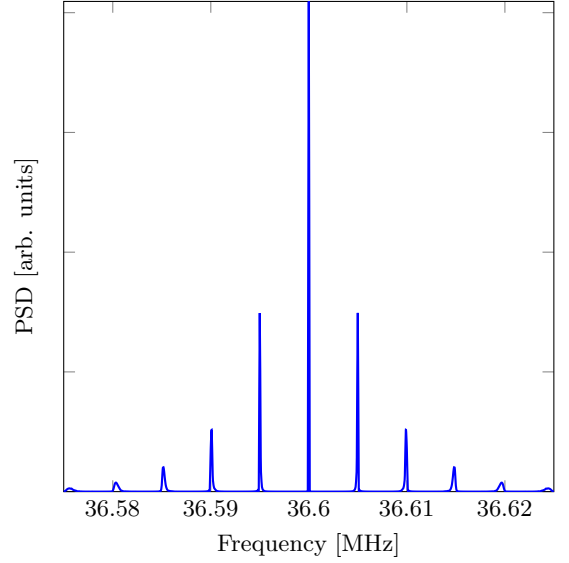
FIG. 1: Simulated longitudinal Schottky spectrum of  $10^4$  macro-particles at the 8th harmonic of the revolution frequency at 5 MHz.

sented respectively by

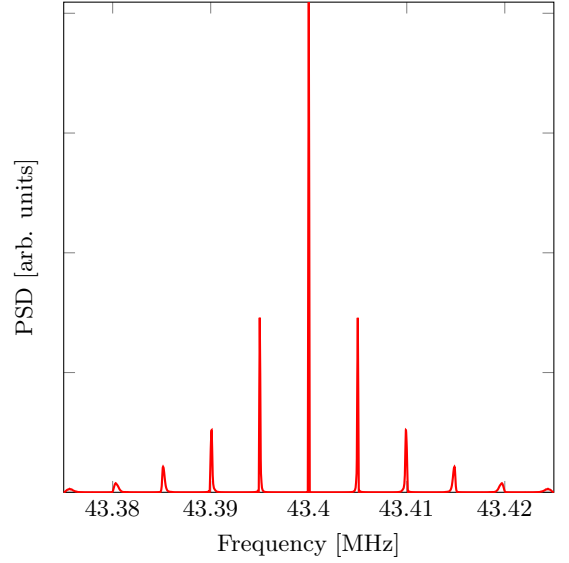
$$\begin{aligned}
 D_{-q}(t) &= \hat{x}_i e f_0 \sum_{i=1}^N \cos \left( (n-q)\omega_0 t + \right. \\
 &\quad \left. (n\hat{\tau}_i - \frac{\hat{Q}_i}{\Omega_{s_i}})\omega_0 \sin(\Omega_{s_i} t + \psi_i) - \phi_i \right) \quad (4) \\
 &= \hat{x}_i e f_0 \sum_{p=-\infty}^{\infty} J_p \left( (n\hat{\tau}_i - \frac{\hat{Q}_i}{\Omega_{s_i}})\omega_0 \right) \\
 &\quad \cos \left( (n-q)\omega_0 t + p\Omega_{s_i} t + p\psi_i - \phi_i \right), \quad (5)
 \end{aligned}$$

$$\begin{aligned}
 D_{+q}(t) &= \hat{x}_i e f_0 \sum_{i=1}^N \cos \left( (n+q)\omega_0 t + \right. \\
 &\quad \left. (n\hat{\tau}_i + \frac{\hat{Q}_i}{\Omega_{s_i}})\omega_0 \sin(\Omega_{s_i} t + \psi_i) + \phi_i \right) \quad (6) \\
 &= \hat{x}_i e f_0 \sum_{p=-\infty}^{\infty} J_p \left( (n\hat{\tau}_i + \frac{\hat{Q}_i}{\Omega_{s_i}})\omega_0 \right) \\
 &\quad \cos \left( (n+q)\omega_0 t + p\Omega_{s_i} t + p\psi_i + \phi_i \right), \quad (7)
 \end{aligned}$$

where  $\hat{x}_i$  is the betatron oscillation amplitude,  $q$  is the fractional part of the nominal fractional tune, and  $\hat{Q}_i = Q\xi\frac{\hat{p}_i}{p_0}$  is the amplitude of the tune oscillations [10], which may have any sign. Here,  $\xi$  represents the chromaticity,  $Q$  is the nominal fractional tune, and  $\hat{p}_i$  is the amplitude of momentum oscillation. The initial betatron phase of particle  $i$ ,  $\phi_i$ , is also drawn from a uniform distribution over the range  $(-\pi, \pi)$ , similar to  $\psi_i$ . The transverse spectrum shape of  $10^4$  macro-particles power spectral density (PSD) under SAPT conditions is shown in Fig. 2.



(a)



(b)

FIG. 2: Simulated PSD of the dipole moment for  $10^4$  macro-particles at the 8th harmonic of the revolution frequency at 5 MHz. Typical SAPT values for betatron tune, synchrotron amplitude, and chromaticity are assumed.

### C. Pre-Simulation Considerations

We selected the resonant stripline BPM [11–15] to detect the Schottky signal from SAPT, with a bandwidth of 3 MHz, an output power of at least  $3.8 \times 10^{-16}$  W, and a sensitivity better than  $2 \Omega/\text{mm}$ . The central frequency of the BPM is yet to be determined. The detected signal from SAPT will first pass through an anti-aliasing filter to exclude frequency components outside the detector's bandwidth. It will then undergo bandpass sampling at a

sampling rate  $f_{\text{sampling}}$ , which is significantly lower than the Nyquist frequency. The details of selecting an appropriate sampling rate will be discussed in Section III A. In the scope of this paper, the central frequency of the BPM is set to 40 MHz.

To reduce computational load and calculation time, the simulation results will include only the frequency components within the detector's bandwidth. This approach facilitates subsequent SNR calculations and noise incorporation in Section II D. Consequently, at each revolution frequency  $f_0$ , all harmonics within the bandwidth can be represented by

$$n \in \{x \in \mathbb{Z} \mid \lceil f_L/f_0 \rceil \leq x \leq \lfloor f_H/f_0 \rfloor\}, \quad (8)$$

where  $\lceil k \rceil$  represents the smallest integer greater than  $k$ , and  $\lfloor k \rfloor$  represents the largest integer smaller than  $k$ . The central frequency of longitudinal and transverse signals at the  $n$ -th harmonic is given by:

$$f_n = n f_0 \quad (9)$$

$$f_{n \pm q} = (n \pm q) f_0 \quad (10)$$

Prior to simulation, any longitudinal or transverse signal component whose central frequency is not within the bandwidth of the detector will be excluded, and only the remaining signal components will be computed. The purpose of the above set is to facilitate simulation; however, in actual operation, the set may differ slightly. The details will be discussed in Section IV A.

In theory, the total power spectral density  $P$  can be expressed as the sum of individual particle contributions  $P_i$ :

$$P = \sum_{i=1}^N P_i \quad (11)$$

due to the random synchrotron and betatron phases of each particle. In practice, we cannot simply sum the time-domain simulation results from  $N$  particles, as the data may exhibit coherence even though they ideally should not, which could affect the calculated power spectral density  $P$ . Besides, in Formula (2), for  $p$ -zeros satellite of the longitudinal signal at harmonic  $n$ , every particle shares the same frequency  $\Omega = n\omega_0$ , but with different amplitudes  $J_0(n\omega_0\hat{\tau}_i)$  and potentially different signs. Summation could lead to this term being smaller than predicted by theory, or even causing it to vanish. Furthermore, the transverse signal spectrum may be significantly distorted.

Considering the above factors, the simulation result will be a matrix of size  $N \times N_t$ , where  $N_t = f_{\text{sampling}} \cdot t$  represents the total number of points for time  $t$  at a sampling rate of  $f_{\text{sampling}}$ .

#### D. Incorporating Simulated Signal into Actual Noise

From the ADC, we collected real noise  $\eta$  with no signal input. The power of a signal  $x$  can be calculated by:

$$P = \frac{1}{N_t} \sum_{i=1}^{N_t} x^2[i]. \quad (12)$$

Then we calculate  $P_{\text{noise}}$ , and subsequently compute the power of the simulated signal,  $P_s$ . The signal-to-noise ratio is defined as:

$$\text{SNR}_{\text{dB}} = 10 \log_{10} \frac{P_{\text{st}}}{P_{\text{noise}}}, \quad (13)$$

where  $P_{\text{st}}$  represents the target power of the simulated signal, yielding:

$$P_{\text{st}} = 10^{\text{SNR}_{\text{dB}}/10} P_{\text{noise}}. \quad (14)$$

Subsequently, the ratio  $k$  between  $P_{\text{st}}$  and  $P_s$  can be calculated by:

$$k = \frac{P_{\text{st}}}{P_s}. \quad (15)$$

Since each particle is incoherent with others, as well as with the noise, the resulting signal after adding the simulated signal to the noise can be expressed as:

$$s' = \sqrt{k} \cdot s + \frac{\eta}{\sqrt{N}}. \quad (16)$$

This process is applied to each particle, for a total of  $N$  particles.

### III. CRITERIA FOR PARAMETER SELECTION

#### A. Sampling Rate

The detector operates at the central frequency  $f_c$  with a lower cutoff frequency  $f_L$  and an upper cutoff frequency  $f_H$ . When the signal is sampled according to the Nyquist–Shannon sampling theorem, the frequency range  $(0, f_L)$  remains unused, thereby limiting both spectrum utilization efficiency and frequency resolution. To address this, bandpass sampling is applied.

For a bandpass signal within  $(f_L, f_H)$ , to sample at a rate lower than the Nyquist frequency without incurring aliasing, the sampling rate  $f_s$  should meet the following conditions [16]:

$$\frac{2f_H}{m+1} \leq f_s \leq \frac{2f_L}{m}, \quad (17)$$

where

$$m \leq \left\lfloor \frac{f_L}{f_H - f_L} \right\rfloor, \quad m \in \mathbb{N}^+. \quad (18)$$

It should be noted that the bandpass sampling procedure maps the frequency  $f$  to:

$$f' = |f - af_s|, \quad (19)$$

where  $a = \text{round}\left(\frac{f_L}{f_s}\right)$ . In the following betatron tune measurements,  $f'$  will be mapped back to  $f$  for calculation convenience.

## B. STFT Window Length

SAPT, designed for proton therapy, is a ramping synchrotron in which the kinetic energy of protons rises from 70 MeV to 235 MeV within 0.35 seconds, corresponding to an increase in the revolution frequency from 4 MHz to 7.5 MHz, with a rate of change of 10 MHz/s. Consequently, there is no period of stable revolution frequency for betatron tune measurement, limiting the frequency resolution.

To measure the betatron tune under these conditions, the Short-Time Fourier Transform (STFT) is employed, assuming that the revolution frequency and beam properties remain constant within each time window. However, this assumption precludes arbitrary selection of the time window length. If the time window is too short, the tune measurement may yield inaccurate results under low SNR conditions due to insufficient spectral resolution. Conversely, if the time window is too long, the rapid variation in revolution frequency becomes significant, resulting in a shift in the position of the transverse signal spectrum.

For a time window length of  $t$  seconds in STFT, the offset of the center location of the sideband between 0 seconds and  $t$  seconds can be denoted as  $f_w$ . During tune measurements, the results are likely to fall within a range centered at  $f_w/2$ , meaning the value of  $f_w$  affects the precision of the measurement. To balance accuracy and precision, a time window length of 1 ms is selected.

## IV. BETATRON TUNE MEASUREMENT PROCEDURE

In previous studies, three primary methods have been employed to identify the betatron tune [3, 5, 9]. The first method, peak detection, identifies the betatron tune by locating the  $p$ -zero satellite. The second method uses spectrum fitting, where an appropriate fitting function is applied to extract the tune. The third approach, the Mirrored Difference method, exploits the coherence between the power of the left and right Bessel  $p$ -satellites to determine the actual center of the sidebands. However, this method is unsuitable for SAPT due to the continuously varying revolution frequency in ramping synchrotrons, which precludes achieving the high frequency resolution needed to resolve the internal structure of Bessel satellites.

Simulation experiments in Section V reveal that these methods fail to provide satisfactory generalizability and stability under SAPT conditions, particularly in scenarios with low SNR and limited frequency resolution. To address these limitations, we propose a novel method specifically tailored for tune measurements in ramping synchrotrons, designed to improve precision, accuracy, and stability in challenging low-SNR environments with constrained frequency resolution. The detailed procedure of the proposed method is presented in this section.

### A. Longitudinal Signal Exclusion

After calculating the signal spectrum, several preprocessing steps are required. The proposed method focuses exclusively on the transverse signal. The revolution frequency is either obtained from other BPMs or calculated independently within the same FPGA using data from other BPMs. Since the longitudinal signal component is not relevant in this context, it is excluded beforehand.

As the kinetic energy of protons may vary, the harmonics of the revolution frequency can appear anywhere within the detector's bandwidth, including near the lower and upper limits. This necessitates predicting the locations of longitudinal signal harmonics near the edges of the detector's bandwidth based on the revolution frequency, so that they can be excluded accordingly. After obtaining the revolution frequency  $f_0$ , we focus on the longitudinal signal at harmonics where:

$$n \in \{x \in \mathbb{Z} \mid \lfloor f_L/f_0 \rfloor \leq x \leq \lceil f_H/f_0 \rceil\}. \quad (20)$$

Our proposed solution to this situation is to calculate the frequency range covered by the longitudinal signal spectrum at each harmonic  $n$ . If there is an overlap with the detector bandwidth, the overlapping portion of the spectrum is set to zero, as illustrated in Fig. 3.

### B. Spectrum Smoothing

After excluding longitudinal signal spectrum, a smoothing procedure is applied to mitigate the impact of noise power, which would otherwise degrade the spectrum and hinder accurate identification of the transverse Schottky signal's shape and position. To extract the transverse signal spectrum, buried within noise, while minimizing the number of data processing batches, several smoothing methods can be employed: Gaussian filtering, locally weighted scatterplot smoothing (LOWESS) [17], and Savitzky-Golay filtering [18, 19]. All these methods require the selection of an appropriately sized window.

When selecting the window size for filtering, manual selection reduces the generalizability of the method. A fixed-length window may produce varying effects depending on the frequency resolution. At low resolution, it



FIG. 3: Comparison of the simulated signal spectrum (blue), noisy spectrum (red), and the spectrum after excluding the longitudinal signal component (green). The spectrum is simulated at a revolution frequency of 6.4 MHz to illustrate the exclusion of the longitudinal signal component. Typical SAPT values, as in Fig. 2, are assumed.

may smooth out the entire transverse signal. Therefore, the window size is determined based on the number of points in the spectrum that encompass the transverse signal spectrum.

This process begins with calculating the widths of the transverse signal spectra. The bandwidth of the transverse spectrum of particle  $i$  is given by [20]:

$$\text{BW}_{\pm T_i} = 2\omega_0 \left| n\hat{\tau} \pm \frac{\hat{Q}}{\Omega_s} \right| \Omega_s. \quad (21)$$

The line width between two adjacent transverse signal spectra is given by:

$$\Delta f_{\pm T} = f_0 \frac{\Delta p}{p} |(n \pm q)\eta \pm Q\xi|, \quad (22)$$

where  $\eta$  is slip factor,  $q$  is the fractional part of betatron tune  $Q$ .

For a bunched beam, the approximate width of the transverse signal spectrum at the  $n$ -th harmonic is:

$$\begin{aligned} \text{BW}_{\pm T} &= \text{BW}_{\pm T_i} + \Delta f_{\pm T} \\ &= 2\omega_0 \left| n\hat{\tau} \pm \frac{\hat{Q}}{\Omega_s} \right| \Omega_s + f_0 \frac{\Delta p}{p} |(n \pm q)\eta \pm Q\xi|. \end{aligned} \quad (23)$$

Given that the detector operates at the central frequency  $f_c$ , the width of the transverse signal spectrum covered by the bandwidth can be calculated. The maximum of these values  $\text{BW}_T$  is selected as the global width of the transverse signal spectra to minimize repeated calculations. Given the frequency resolution  $\Delta f$ , the

number of points covering the transverse Schottky signal spectrum can be derived as:

$$N_T = \left\lceil \frac{\Delta f}{\text{BW}_T} \right\rceil. \quad (24)$$

Experimental results under varying sampling rates and revolution frequencies indicate that optimal smoothing is achieved when the window size  $N_f$  is set to:

$$N_f = \max\left(3, 2 \left\lceil \frac{N_T}{4} \right\rceil - 1\right). \quad (25)$$

The STFT time window, containing  $N_t$  points, will be divided into multiple batches for performing the FFT, with each batch containing  $N_b$  frequency bins. For the PSD of a single batch, the calculated window size is applied for smoothing, and the results are shown in Fig. 4.

After applying smoothing techniques, the following metric is computed:

$$P_{\text{prod}} = \prod P_{b_i}, \quad (26)$$

where  $P_{b_i}$  represents the power spectral density of batch  $i$ .

The rationale for calculating the product of the spectrum of batches is that, over a very short time interval, the properties of bunched beam, such as revolution frequency and betatron tune, can be assumed to remain constant. Therefore, in the power spectral density of each batch, the sideband will appear in the same position and with the same shape, though subject to random fluctuations due to noise. This consistency allows the spectrum from one batch to be used as a filter for the next. The

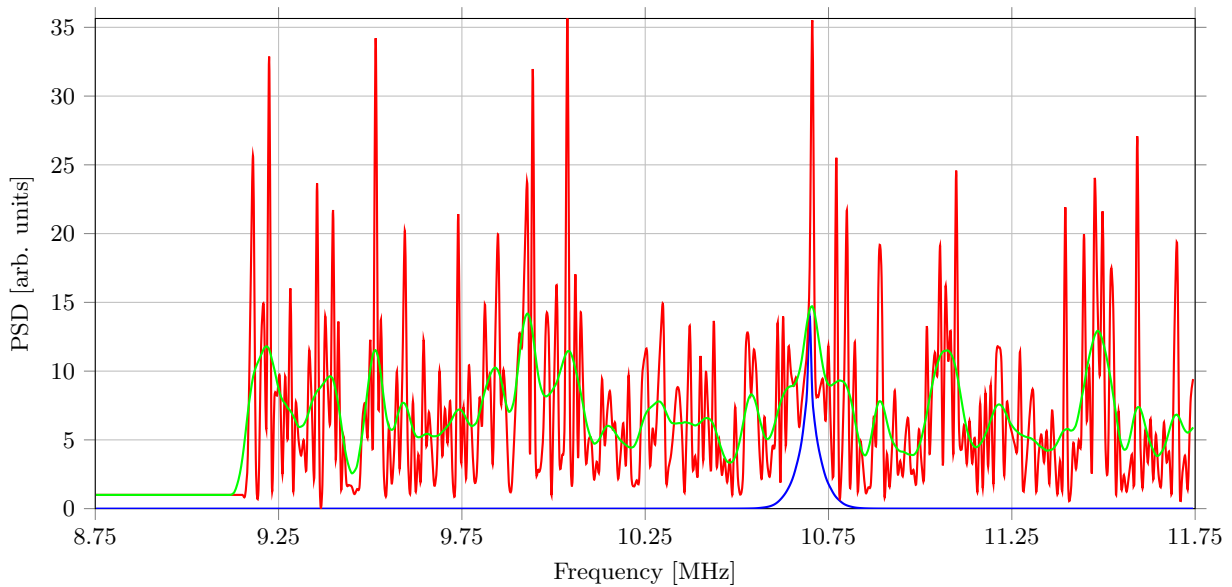


FIG. 4: Comparison between the simulated spectrum (blue), the noisy spectrum (red), and the smoothed spectrum obtained using Gaussian filter (green). Same beam properties, as in Fig. 3, are assumed.

noise spectrum is suppressed, while the sidebands are enhanced.

The transverse signal is not prominent in the spectrum of the first batch, as shown in Fig. 5a; however, as more batches are multiplied, it gradually emerges and becomes significant, as shown in Fig. 5h.

### C. Tune Calculation

After calculating  $P_{\text{prod}}$ , its maximum is identified, and the surrounding  $N_T/2$  points, along with their corresponding frequencies, are selected for a curve fitting procedure. The choice of  $N_T/2$  points, rather than  $N_T$ , is based on the observation that the multiplication across multiple batches narrows the width of the sidebands. In practice,  $N_T/2$  points provide a suitable balance for accurate curve fitting. The fitting function is a Gaussian distribution, expressed as:

$$f(x) = a \exp\left(-\frac{(x - b')^2}{2c^2}\right), \quad (27)$$

where  $a$  is the peak amplitude,  $b'$  represents the location of the peak, and  $c$  determines the width of the distribution. The fitted peak coordinate  $b'$  is subsequently mapped back to its actual frequency  $b$ , as described in Section III A. The fractional tune  $q$  is then defined as:

$$q = b/f_0 - [b/f_0], \quad (28)$$

or as:

$$q = 1 - b/f_0 + [b/f_0], \quad (29)$$

depending on the specific context.

## V. EXPERIMENTS

The experiments were designed to evaluate and compare the performance of the proposed betatron tune measurement method against previously established methods [3, 5] under SAPT conditions. To achieve this, SAPT design parameters were used for a 0.35 s Monte Carlo macro-particle simulation based on the time-domain formulas (1), (4), and (6), with a revolution frequency linearly increasing from 4 MHz to 7.5 MHz and an STFT time window size of 1 ms. The simulated data were then combined with real noise from the ADC to emulate practical measurement conditions. Sections V A, V B, and V C investigate the effects of SNR, sampling rate, and the number of frequency bins to assess the general applicability of the proposed method. These sections compare three key metrics for both the proposed and existing methods: (1) the average absolute error of the measured tune relative to the nominal fractional tune, reflecting precision and accuracy; (2) the standard deviation of the measured tune, indicating stability; and (3) the percentage of measured tunes falling within  $q \pm 0.001$ , evaluating compliance with design requirements. By varying one parameter while keeping the others constant, this analysis provides a comprehensive evaluation of the proposed method's performance relative to existing approaches, showcasing its advantages in terms of precision, accuracy, and stability under challenging conditions.

### A. Impact of SNR Variations

In this scenario, the number of frequency bins and the sampling rate are fixed at 4096 and 29.75 MHz, respec-

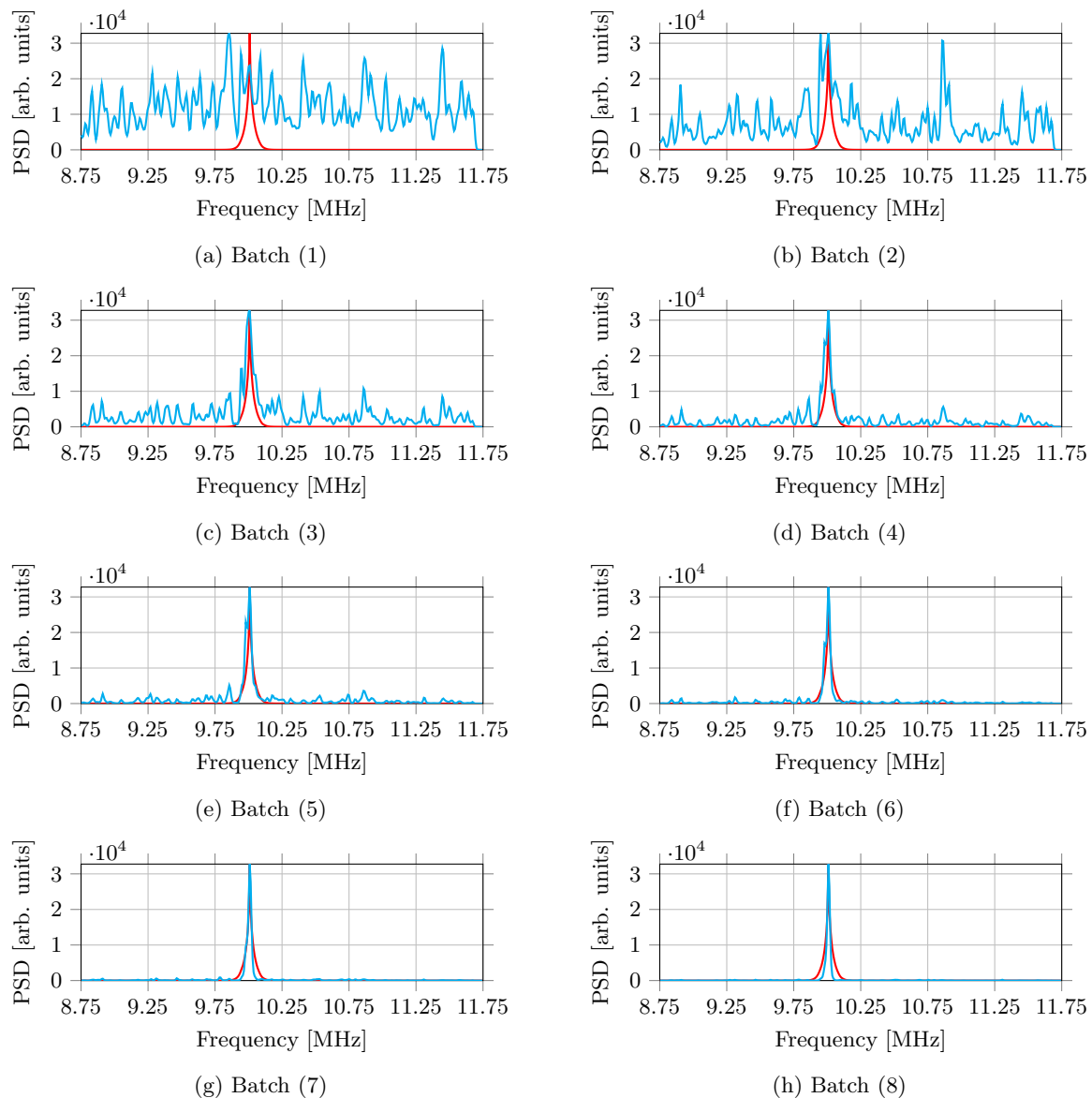


FIG. 5: Comparison between the simulated signal (red), the product  $P_{\text{prod}}$  (cyan) of multiple spectra within the STFT time window.

tively, while the SNR is evaluated at  $-15$  dB,  $-10$  dB, and  $-5$  dB. The average absolute error ( $\mu$ ) of the measured tune relative to the nominal fractional tune  $q$ , the standard deviation ( $\sigma$ ) of the measured tune, and the percentage of measured tunes falling within  $q \pm 0.001$  ( $P_{q \pm 0.001}$ ) for different betatron tune measurement methods are summarized in Table I.

### B. Impact of Sampling Rate Variations

In this scenario, the SNR and number of frequency bins are fixed at  $-15$  dB and 4096, respectively, while sampling rates of 17.00 MHz, 29.75 MHz, and 50.00 MHz are evaluated. The average absolute error ( $\mu$ ) of measured

tune relative to the nominal fractional tune  $q$ , standard deviation ( $\sigma$ ) of measured tune, and the percentage of measured tunes falling within  $q \pm 0.001$  ( $P_{q \pm 0.001}$ ) for different betatron tune measurement methods are summarized in Table II.

### C. Impact of Frequency Bin Variations

In this scenario, the SNR and sampling rate are fixed at  $-15$  dB and 29.75 MHz, respectively, while the number of frequency bins of 2048, 4096 and 8192 are evaluated. The average absolute error ( $\mu$ ) of measured tune relative to the nominal fractional tune  $q$ , the standard deviation ( $\sigma$ ) of measured tune, and the percentage of measured tunes

TABLE I: Comparison of the average absolute error ( $\mu$ ) of the measured tune relative to the nominal fractional tune  $q$ , standard deviation ( $\sigma$ ) of the measured tune, and the percentage of measured tunes falling within  $q \pm 0.001$  ( $P_{q \pm 0.001}$ ) for different betatron tune measurement methods. The comparison is performed under SNR values of -15 dB, -10 dB, and -5 dB, with 4096 frequency bins and a sampling rate of 29.75 MHz. For ease of comparison, the values of  $\mu$  and  $\sigma$  are scaled by  $10^4$ .

SNR	Method	$\mu$	$\sigma$	$P_{q \pm 0.001}$ (%)
-15 dB	Peak Detection [3]	6.24	7.94	78.57
	Curve Fitting [3, 5]	5.48	6.90	83.67
	Proposed Method (Savitzky-Golay Filter)	3.98	5.02	94.56
	Proposed Method (LOWESS)	4.24	5.59	93.54
	Proposed Method (Gaussian Filter)	3.15	4.12	96.94
-10 dB	Peak Detection [3]	3.52	4.29	98.30
	Curve Fitting [3, 5]	1.59	2.01	100.00
	Proposed Method (Savitzky-Golay Filter)	1.50	1.81	100.00
	Proposed Method (LOWESS)	3.19	4.19	96.60
	Proposed Method (Gaussian Filter)	1.12	1.40	100.00
-5 dB	Peak Detection [3]	3.18	3.76	100.00
	Curve Fitting [3, 5]	0.63	0.79	100.00
	Proposed Method (Savitzky-Golay Filter)	0.64	0.80	100.00
	Proposed Method (LOWESS)	4.99	6.27	88.10
	Proposed Method (Gaussian Filter)	0.69	0.86	100.00

TABLE II: Comparison of the average absolute error ( $\mu$ ) of measured tune relative to the nominal fractional tune  $q$ , the standard deviation ( $\sigma$ ) of measured tune, and the percentage of measured tunes falling within  $q \pm 0.001$  ( $P_{q \pm 0.001}$ ) for different betatron tune measurement methods. The comparison is performed under sampling rates of 17.00 MHz, 29.75 MHz and 50.00MHz, with 4096 frequency bins and an SNR of -15 dB. For ease of comparison, the values of  $\mu$  and  $\sigma$  are scaled by  $10^4$ .

Sampling Rate	Method	$\mu$	$\sigma$	$P_{q \pm 0.001}$ (%)
17.00 MHz	Peak Detection [3]	7.17	11.42	75.51
	Curve Fitting [3, 5]	8.88	63.54	86.73
	Proposed Method (Savitzky-Golay Filter)	4.50	5.65	92.86
	Proposed Method (LOWESS)	4.77	6.20	89.80
	Proposed Method (Gaussian Filter)	4.17	5.44	92.86
29.75 MHz	Peak Detection [3]	11.92	100.93	81.29
	Curve Fitting [3, 5]	10.93	100.88	87.07
	Proposed Method (Savitzky-Golay Filter)	3.97	5.06	96.26
	Proposed Method (LOWESS)	3.85	5.11	93.88
	Proposed Method (Gaussian Filter)	3.46	4.40	97.28
50.00 MHz	Peak Detection [3]	37.67	208.88	77.21
	Curve Fitting [3, 5]	36.68	209.10	80.95
	Proposed Method (Savitzky-Golay Filter)	3.60	4.89	96.94
	Proposed Method (LOWESS)	3.18	4.30	96.60
	Proposed Method (Gaussian Filter)	3.44	4.50	97.28

falling within  $q \pm 0.001$  ( $P_{q \pm 0.001}$ ) for different betatron tune measurement methods are summarized in Table III.

#### D. Results Discussion

Based on the experimental results presented in Sections V A, V B, and V C, the proposed method employ-

ing the Gaussian filter demonstrates robust performance, achieving the lowest average absolute error relative to the nominal fractional tune  $q$  and the smallest standard deviation in most scenarios, thereby exhibiting strong general applicability and stability. The Savitzky-Golay filter-based variant of the proposed method follows closely in performance but incurs greater computational complexity due to its reliance on polynomial fitting, which has a

TABLE III: Comparison of the average absolute error ( $\mu$ ) of measured tune relative to the nominal fractional tune  $q$ , the standard deviation ( $\sigma$ ) of measured tune, and the percentage of measured tunes falling within  $q \pm 0.001$  ( $P_{q \pm 0.001}$ ) for different betatron tune measurement methods. The comparison is performed under 2048, 4096 and 8192 frequency bins, with a sampling rate of 29.75 MHz and an SNR of -15 dB. For ease of comparison, the values of  $\mu$  and  $\sigma$  are scaled by  $10^4$ .

Frequency bins	Method	$\mu$	$\sigma$	$P_{q \pm 0.001}$ (%)
2048	Peak Detection [3]	21.65	156.14	76.53
	Curve Fitting [3, 5]	19.75	156.12	85.37
	Proposed Method (Savitzky-Golay Filter)	3.68	4.63	97.62
	Proposed Method (LOWESS)	3.67	4.58	96.94
	Proposed Method (Gaussian Filter)	3.71	4.73	96.26
4096	Peak Detection [3]	6.00	7.55	79.93
	Curve Fitting [3, 5]	5.05	6.49	89.12
	Proposed Method (Savitzky-Golay Filter)	3.88	4.90	94.90
	Proposed Method (LOWESS)	4.03	5.17	94.22
	Proposed Method (Gaussian Filter)	3.17	4.16	97.96
8192	Peak Detection [3]	6.54	8.48	78.23
	Curve Fitting [3, 5]	5.27	6.74	85.71
	Proposed Method (Savitzky-Golay Filter)	4.12	5.30	94.22
	Proposed Method (LOWESS)	5.08	6.74	87.76
	Proposed Method (Gaussian Filter)	3.60	4.52	96.60

computational complexity of  $O(N_b N_f M^3)$  [21], where  $M$  represents the polynomial order. In contrast, the Gaussian filter operates through weighted averaging, with a reduced computational complexity of  $O(N_b N_f)$ . Consequently, the proposed method with the Gaussian filter achieves superior precision and accuracy while requiring fewer computational resources.

## VI. CONCLUSION

In this paper, we proposed a Schottky diagnostics-based method for real-time betatron tune measurement in the SAPT ramping synchrotron, addressing key challenges such as low SNR, varying revolution frequency, limited frequency resolution and fluctuating betatron tune. By employing macro-particle Monte Carlo simulations and incorporating real-world noise, we demonstrated the effectiveness of the method in extracting transverse Schottky signals buried within noise. Utilizing STFT alongside advanced smoothing and spectrum processing techniques, the proposed approach achieved

precise betatron tune measurements under diverse experimental conditions.

Experimental results identified the proposed method with the Gaussian filter as the most effective, delivering superior precision and accuracy, thus demonstrating its robustness, general applicability, and stability. The method achieved an average absolute error relative to the nominal fractional tune below 0.001 with a low standard deviation, satisfying the design requirements for high-precision tune diagnostics in ramping synchrotrons. This study provides a foundation for optimizing betatron tune diagnostics in ramping synchrotrons and advancing diagnostic techniques for applications such as proton therapy.

Future work will focus on expanding the operational range of the proposed method and validating its applicability in other synchrotron facilities. Further optimization of computational efficiency will also be pursued to enhance real-time performance in demanding environments.

Additionally, an FPGA-based online implementation of the proposed method is currently in development, aiming to provide high-precision, real-time betatron tune measurements for SAPT.

[1] M.-Z. Zhang, D.-M. Li, L.-R. Shen, H.-R. Zhang, Z.-L. Chen, H.-W. Du, M. Gu, R. Li, D.-K. Liu, Y.-H. Pu, *et al.*, Sapt: a synchrotron-based proton therapy facility in shanghai, Nuclear Science and Techniques **34**, 148 (2023).

[2] S. van der Meer, *Stochastic damping of betatron oscillations in the SIS*, Tech. Rep. (CERN, Geneva, 1972).

[3] M. Betz, O. Jones, T. Lefevre, and M. Wendt, Bunched-beam schottky monitoring in the lhc, Nuclear Instruments and Methods in Physics Research Section A: Accelerators, Spectrometers, Detectors and Associated Equipment **874**, 113 (2017).

[4] S. van der Meer, *Diagnostics with Schottky noise*, Tech. Rep. (CERN, Geneva, 1988).

- [5] O. Chanon, *Schottky signal analysis: tune and chromaticity computation*, Tech. Rep. (2016).
- [6] K. Lasocha and D. Alves, Estimation of longitudinal bunch characteristics in the lhc using schottky-based diagnostics, *Physical Review Accelerators and Beams* **23**, 062803 (2020).
- [7] C. Lannoy, D. Alves, K. Lasocha, N. Mounet, and T. Pieloni, Lhc schottky spectrum from macro-particle simulations, in *11th International Beam Instrumentation Conference* (JACoW Publishing, 2022) pp. 308–312.
- [8] K. Lasocha, D. Alves, C. Lannoy, N. Mounet, and T. Pieloni, Extraction of LHC Beam Parameters from Schottky Signals, *JACoW HB* **2023**, 382 (2024).
- [9] K. Lasocha and D. Alves, Estimation of transverse bunch characteristics in the lhc using schottky-based diagnostics, *Physical Review Accelerators and Beams* **25**, 062801 (2022).
- [10] K. Lasocha, *Non-Invasive Beam Diagnostics with Schottky Signals and Cherenkov Diffraction Radiation*, Ph.D. thesis (2022).
- [11] B. Keil, A. Citterio, M. Dehler, R. Ditter, V. Schlott, L. Schulz, and D. Treyer, Commissioning of the low-charge resonant stripline bpm system for the swissfel test injector, in *Proc. FEL* (2010) p. 429.
- [12] T. Petersen, J. Diamond, N. Liu, P. Prieto, D. Slimmer, and A. Watts, Fermilab switchyard resonant beam position monitor electronics upgrade results, arXiv preprint arXiv:1701.00816 (2017).
- [13] A. Citterio, M. Dehler, D. Treyer, B. Keil, V. Schlott, and L. Schulz, Design of a resonant stripline beam position pickup for the 250mev psi xfel test injector, in *Proc. DIPAC*, Vol. 9 (2009).
- [14] M. Dehler, Resonant strip line bpm for ultra low current measurements, in *Proc. DIPAC*, Vol. 5 (2005) p. 284.
- [15] M. Kesselman, P. Cameron, and J. Cupolo, Resonant bpm for continuous tune measurement in rhic, in *PACS2001. Proceedings of the 2001 Particle Accelerator Conference (Cat. No. 01CH37268)*, Vol. 2 (IEEE, 2001) pp. 1357–1359.
- [16] R. G. Vaughan, N. L. Scott, and D. R. White, The theory of bandpass sampling, *IEEE Transactions on signal processing* **39**, 1973 (1991).
- [17] W. S. Cleveland, Robust locally weighted regression and smoothing scatterplots, *Journal of the American statistical association* **74**, 829 (1979).
- [18] A. Savitzky and M. J. Golay, Smoothing and differentiation of data by simplified least squares procedures., *Analytical chemistry* **36**, 1627 (1964).
- [19] R. W. Schafer, What is a savitzky-golay filter?[lecture notes], *IEEE Signal processing magazine* **28**, 111 (2011).
- [20] D. Boussard, *Schottky noise and beam transfer function diagnostics*, Tech. Rep. (CERN, 1986).
- [21] T. Konstantinovskiy, Introduction to the savitzky-golay filter: A comprehensive guide (using python), *The Pythoneers* (2024), accessed: 2024-12-06.